Journal of Solid State Chemistry 184 (2011) 2339–2344

Contents lists available at ScienceDirect

Journal of Solid State Chemistry

journal homepage: www.elsevier.com/locate/jssc

Fabrication of Cu–Ag core–shell bimetallic superfine powders by eco-friendly reagents and structures characterization

Jun Zhao, Dongming Zhang*, Jie Zhao

State Key Laboratory of Advanced Technology for Materials Synthesis and Processing, Wuhan University of Technology, Yi Fu Building 4th Floor, Wuhan 430070, China

ARTICLE INFO

Article history:
Received 5 January 2011
Received in revised form
22 June 2011
Accepted 26 June 2011
Available online 8 July 2011

Keywords:
Silver
Copper
Cyclodextrins
Core–shell structure

ABSTRACT

Superfine bimetallic Cu–Ag core–shell powders were synthesized by reduction of copper sulfate pentahydrate and silver nitrate with eco-friendly ascorbic acid as a reducing agent and cyclodextrins as a protective agent in an aqueous system. The influence of Ag/Cu ratio on coatings was investigated. Ag was homogeneously distributed on the surface of Cu particles at a mole ratio of Ag/Cu=1. FE–SEM showed an uniformity of Ag coatings on Cu particles. Antioxidation of Cu particles was improved by increasing Ag/Cu ratio. TEM–EDX and UV–vis spectra also revealed that Cu cores were covered by Ag nanoshells on the whole. The surface composition analysis by XPS indicated that only small parts of Cu atoms in the surface were oxidized. It was noted that the hindrance of cyclodextrins chemisorbed on particles plays an important role in forming high quality and good dispersity Cu–Ag (Cu@Ag) core–shell powders.

1. Introduction

Ag and Cu with high electrical conductivity are widely used in the electronic industry [1–3], catalysis [4,5], sensors [6], and optical and biological devices [7–10]. But the rare content of Ag in earth's crust and easy oxidization of Cu strongly constrain their applications. Thus Cu–Ag composite powder instead of single copper or silver powder is currently considered to be a desirable option in electronic industry to solve the above problems [11]. There are many ways to form core–shell composite particles such as electroplating [12], electroless plating [13–15], vacuum process [16], sputtering, etc. Many of these techniques are suited only for laboratory-scale production because of low efficiency or the need of precious equipment. Electroless plating is the most potential process for synthesizing Cu–Ag composites due to its advantages such as simplicity and high efficiency. However, most of the processes used polyvinylpyrrolidone (PVP), hexadecyl trimethyl ammonium bromide (CTAB) and sodium borohydride ($NaBH_4$), hydrazine hydrate ($N_2H_4{\bullet}H_2O$), formaldehyde (HCHO), etc. as dispersant and reductant, respectively, which are noxious or hard to be removed from the final products. In the recent years, cyclodextrins (CDs) have been increasingly used to prepare metal nanoparticles such as gold [17], palladium [18], and platinum[19]. CDs are cyclic oligosaccharides which consist of covalently linked glucose units (6 α-CD units, 7 β-CD units, 8 γ-CD units) and can be characterized by a hydrophilic exterior and a hydrophobic interior [20]. β-CD has also been used to prepare gold and silver nanoparticles in the presence of different reducing agents such as dimethyl formamide, ethanol, methanol, ethylene glycol, and sodium citrate because of its special structure [21–23].

In this paper, a simple chemical reduction method was used to synthesize superfine Cu–Ag powders with β-CDs as an efficient protective agent in a one-step process and the mechanism was explained. As compared with the results reported previously this method is a relatively green synthetic method because the starting materials come from supramolecular β-CDs as protective agents and ascorbic acid (Vc) as the reducing agent, which are nontoxic and easily available. The full-coated Cu powders prepared by this method are good dispersed and hardly oxidized, which have potential applications in many fields.

2. Experimental details

2.1. Materials

Copper sulfate pentahydrate ($CuSO_4{\bullet}5H_2O$), silver nitrate ($AgNO_3$), ascorbic acid ($C_6H_8O_6$), absolute ethyl alcohol (C_2H_6O), β-CDs ($(C_6H_{10}O_5)_7$), ammonia solution, and sodium hydroxide (NaOH) were purchased from Chemical Reagent Co. Ltd., China, and used as received without further purification.

2.2. Preparation of Cu–Ag core–shell particles

About 0.01 mol β-CDs and 150 ml deionized water were heated to dissolve at 40 °C with a magnetic stirrer. Vc amounting to the sum of $CuSO_4{\bullet}5H_2O$ and $AgNO_3$ was put into the solution; then the solution was adjusted to pH=11 using 1 M NaOH. Detailed experiment design was shown in Table 1. The prepared solution was used as a reducing agent. $CuSO_4{\bullet}5H_2O$ and $AgNO_3$ were reacted to form $[Cu(NH_3)_4]^{2+}$

* Corresponding author. Fax: +86 027 87168606.
E-mail address: zhangdongming71@hotmail.com (D. Zhang).

0022-4596/$ - see front matter © 2011 Elsevier Inc. All rights reserved.
doi:10.1016/j.jssc.2011.06.032

Table 1
Proportions and compositions of composite powders.

Sample	$n$$CuSO_4$•$5H_2O$/ $n$$AgNO_3$	$CuSO_4$•$5H_2O$ (mol)	$AgNO_3$ (mol)	Vc (mol)	β-CDs (mol)
1	1:1	0.01	0.01	0.02	0.01
2	2:1	0.01	0.005	0.015	0.01
3	3:1	0.01	0.0033	0.0133	0.01
4	4:1	0.01	0.0025	0.0125	0.01

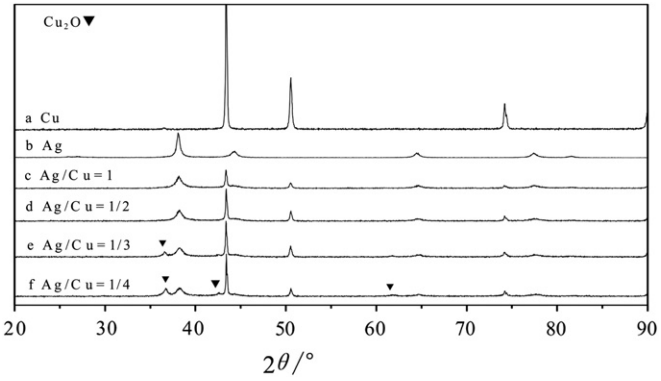

Fig. 1. XRD patterns of particles with different composition ratios.

and $[Ag(NH_3)_2]^+$ by adding excess aqueous ammonia. First, $[Cu(NH_3)_4]^{2+}$ colloids were dropped into the reducing solution at a speed of 60 drops/min at 70 °C. After 20 min, $[Ag(NH_3)_2]^+$ was dropped into the solution at the same speed. The composite powders were obtained when the resulting solution was washed, separated by centrifugation and then dried.

2.3. Characterization

The morphologies of the composite powders were observed by TEM (JEOL Model JEM-2010-HT at 200 kV) and FE–SEM (S-4800, Hitachi, Japan). XRD measurements were performed on a Rigaku D/max III.V X-ray diffractometer using Cu$K\alpha$ radiation (λ=0.1542 nm). XPS measurements were obtained using a Fison (VG) ESCA 210 spectrometer equipped with an Al$K\alpha$ X-ray source. FT-IR spectra were collected using an FTS135 infrared spectroscope. Absorption spectra were recorded in a Shimadzu UV-160 spectrophotometer (Kyoto, Japan) taking the solutions in a 1 cm quartz cuvette.

3. Results and discussion

3.1. Effect of Ag/Cu ratio on Cu–Ag composite powders

XRD analysis was performed to ascertain the crystal structure and composition of the synthetic particles. Fig. 1 shows the XRD

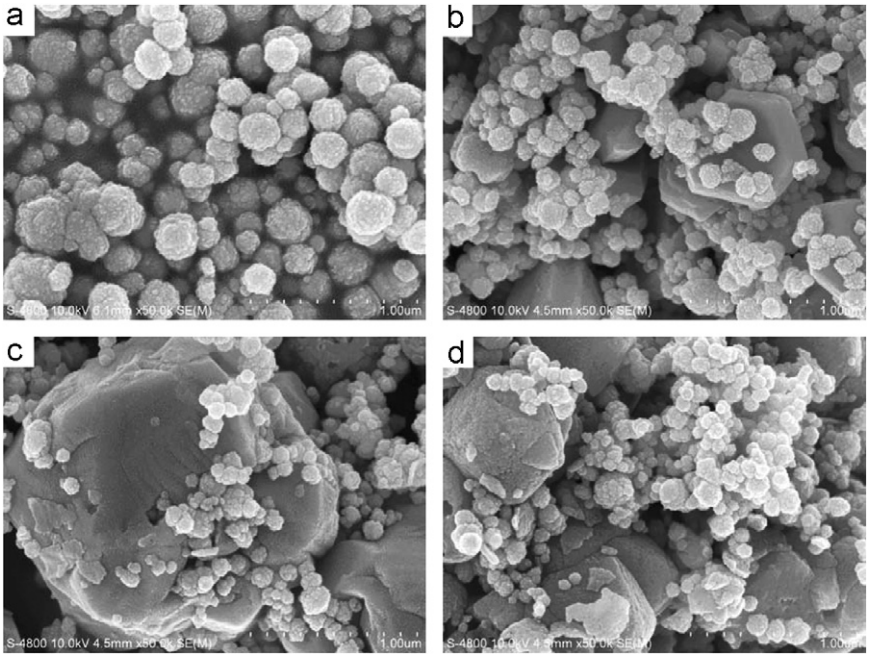

Fig. 2. FE–SEM images of Cu–Ag core–shell particles with [Cu]/[Ag]=(a) 1, (b) 2, (c) 3, and (d) 4.

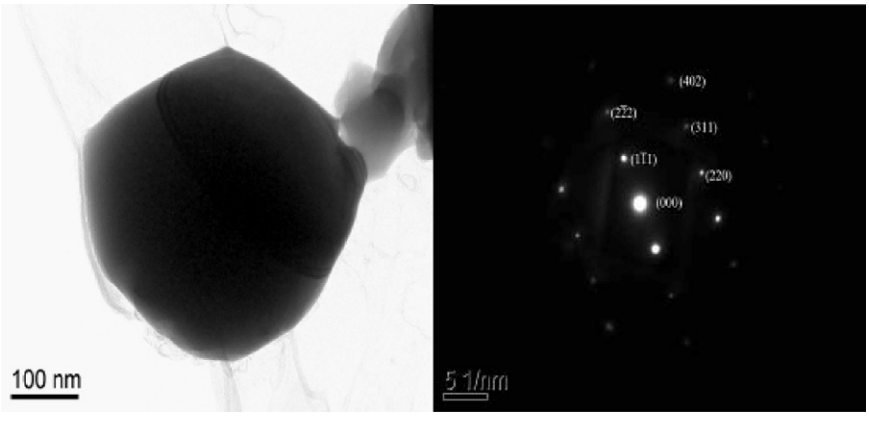

Fig. 3. Diffraction patterns of large regular particles in Specimens 2–4.

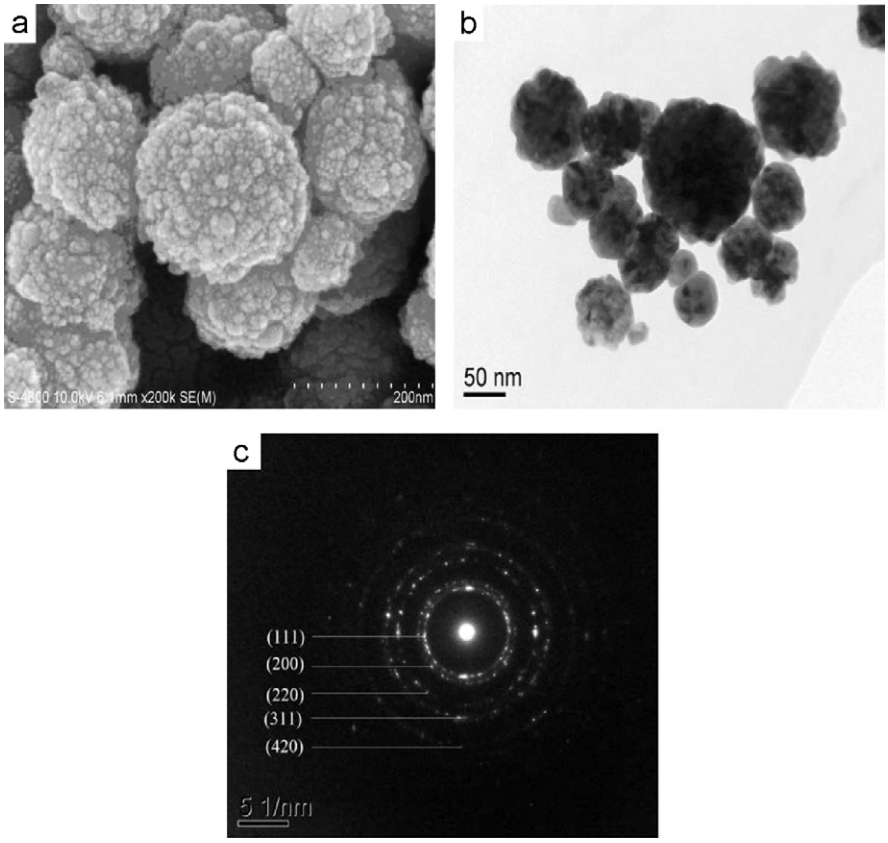

Fig. 4. Selected area electron diffraction analysis of Cu–Ag.

spectra of Cu, Ag, and Cu–Ag powders. In Fig. 1c, both Cu and Ag phases were clearly identified. Also a Cu_2O phase was found in Fig.1 e and f, indicating that Cu was partially oxidized with decreasing Ag/Cu molar ratio. The reason will be discussed later.

Fig. 2 shows the FE–SEM images of Cu–Ag composite particles with different Ag/Cu molar ratios. Two kinds of particles are shown in the images: spherical particles and large irregular ones. It can be seen that the diameters of Cu–Ag composite particles are in the 100–150 nm range at Ag/Cu=1. The composite particles become non-uniform with decreasing Ag/Cu ratio. In Fig. 2b–d, the number of small spherical particles decreased and the amount of large hexagonal particles increased. Further analysis by TEM with diffraction patterns, as shown in Fig. 3, indicates that the large uncovered particles were fcc crystal of copper. Thus, Cu particles were incompletely covered by Ag at molar ratio of Ag/Cu < 1. The Cu particles are easily oxidized into Cu_2O, which was found by XRD in those samples.

3.2. *Characterization of Cu–Ag particles*

The FE–SEM image in Fig. 4a shows the enlarged image of Specimen 1. Many nanoparticles are found on the surface of large spherical particles. The TEM image in Fig. 4b clearly shows that there is a layer of nanoparticles less than 20 nm on the surface. Fig. 4c displays the diffraction rings for the nanoparticles confirming the Ag crystal; only the (1 1 1), (2 0 0), (2 2 0), (3 1 1), and (4 2 0) planes of face-centered cubic (fcc) Ag are shown; no diffraction spot for Cu is found. There may be two reasons for the results: (1) As Ag gradually deposited onto the Cu particles, lattice parameter mismatches occur between Cu and Ag, which hinder the epitaxial growth of Ag on Cu. Thus, an incoherent interface develops between the Cu core and the Ag shell. Due to this incoherent interface, if the Ag shell is in dynamical

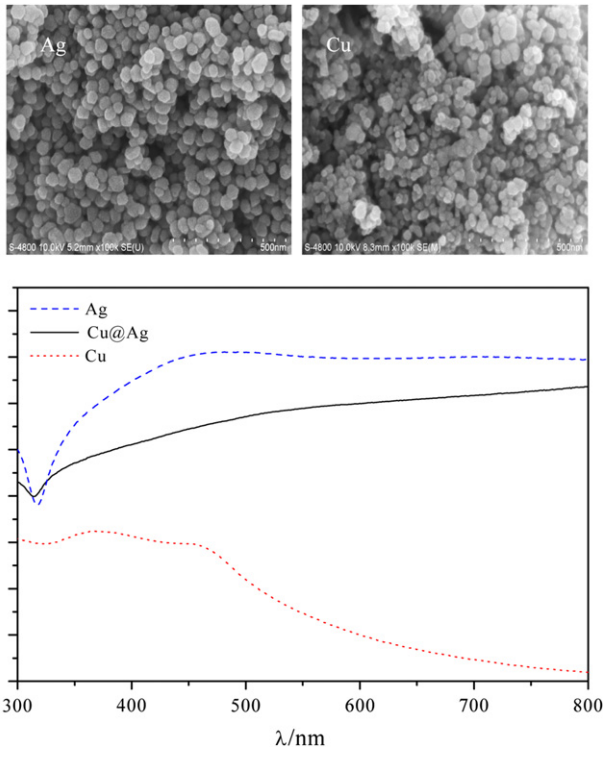

Fig. 5. UV–vis absorption spectra of the Ag, Cu@Ag, and Cu nanoparticles.

diffraction conditions, then the Cu core is in kinematical state. Less diffraction spot from the core Cu is observed in Ag with brighter contrast [24]. (2) Cu mainly lies at the center of the

composite powder (> 100 nm), so it is hard to be transmited to show diffraction spot. Further TEM–EDS result supports the deduction.

As can be seen in Fig. 5b–d by TEM–EDS, the average Ag/Cu ratios for the particle were 6.71, 5.91, and 4.07 from external location 1 to internal location 3. This indicates that the Ag/Cu ratio is larger at point 1 (outside) than at points 2 (interim) and 3 (center). The center of the particle is a Cu-rich area while the edges are Ag-rich areas. Results show that Cu is primarily located in particle centers, but no distinct Ag and Cu region is formed, as shown in Figs. 6a and 4b. The result indicates that crystallization of Cu is imperfect because Cu reduces Ag^{+} spontaneously as described by Eq. (1), and then Cu^{2+} enters into the solution. Cu^{2+} is reduced by Vc to deposit onto Cu surface uncovered by Ag on the large particles as described by Eq. (2). The two steps go on repeatedly until the large particles are covered fully by Ag. If the mount of Cu^{2+} is more than that of Ag^{+} the rest of reduced Cu^{2+} will form large crystal Cu, as found in Fig. 2b–d.

$$Cu + 2Ag^{+} \rightarrow 2Ag + Cu^{2+} \quad (1)$$

$$Cu^{2+} + C_6H_6O_4(OH)_2 \rightarrow Cu + C_6H_6O_6 + 2H^{+} \quad (2)$$

The UV–vis spectrum of the as-prepared Cu–Ag nanoparticles is given in Fig. 6. SEM of Ag and Cu particles about 50 nm used for UV–vis spectrum analysis is also presented in Fig. 6. The adsorption tendency of Ag and Cu–Ag particles increases while that of Cu powders decreases with the increase of wave length. Ag and Cu–Ag particles reveal a similar absorbance tendency, which are different from that of Cu. The result further indicates that the composite particles are Cu@Ag particles.

XPS was also performed to study the surface information of Cu–Ag composites. As seen in Fig. 7a the intensity of Ag peak is higher than that of Cu, which clearly shows that Ag is focused outside the composite particles. This result is in agreement with TEM–EDS findings. Fig. 7c shows that Ag2*p*5/2 (367.901 eV) and Ag2*p*3/2 (374.001 eV) peaks are associated with zero-valent Ag at 368 and 374 eV, respectively. Besides, the good symmetry of Ag peaks proves that the valence of Ag does not change. The major contributions of the Cu2*p*3/2 (932.2 eV) and Cu2*p*1/2 (952 eV) peaks are associated with zero-valent Cu. However the smaller contributions of the two peaks splitting, along with the additional shake-up lines at peaks of 942.6 and 961.7 eV, are consistent with CuO peaks in Fig. 7d. The binding energy of Cu° and Cu^{+} is 932.2 and 932.5 eV, respectively. It is hard to differentiate the states of Cu° and Cu^{+} with the small binding energy difference. So Cu Auger electron signal is used to differentiate Cu° and Cu^{+} in 910–920 eV. The strongest Auger peak of Cu° is at 919.0 eV while that of Cu^{+} is at 916.8 eV. It can be seen from Fig. 7b enlarged

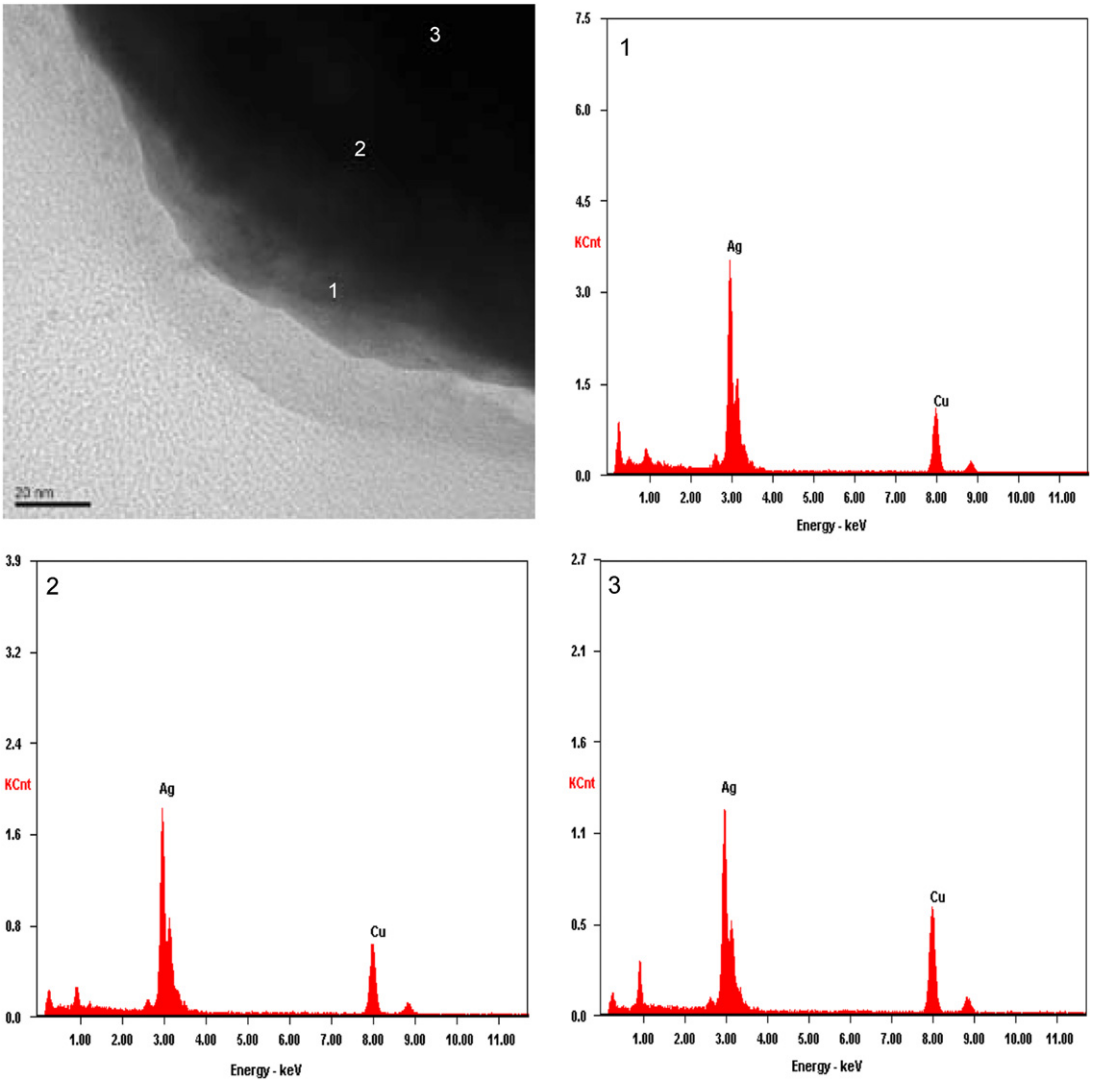

Fig. 6. TEM–EDS image of Cu–Ag particles.

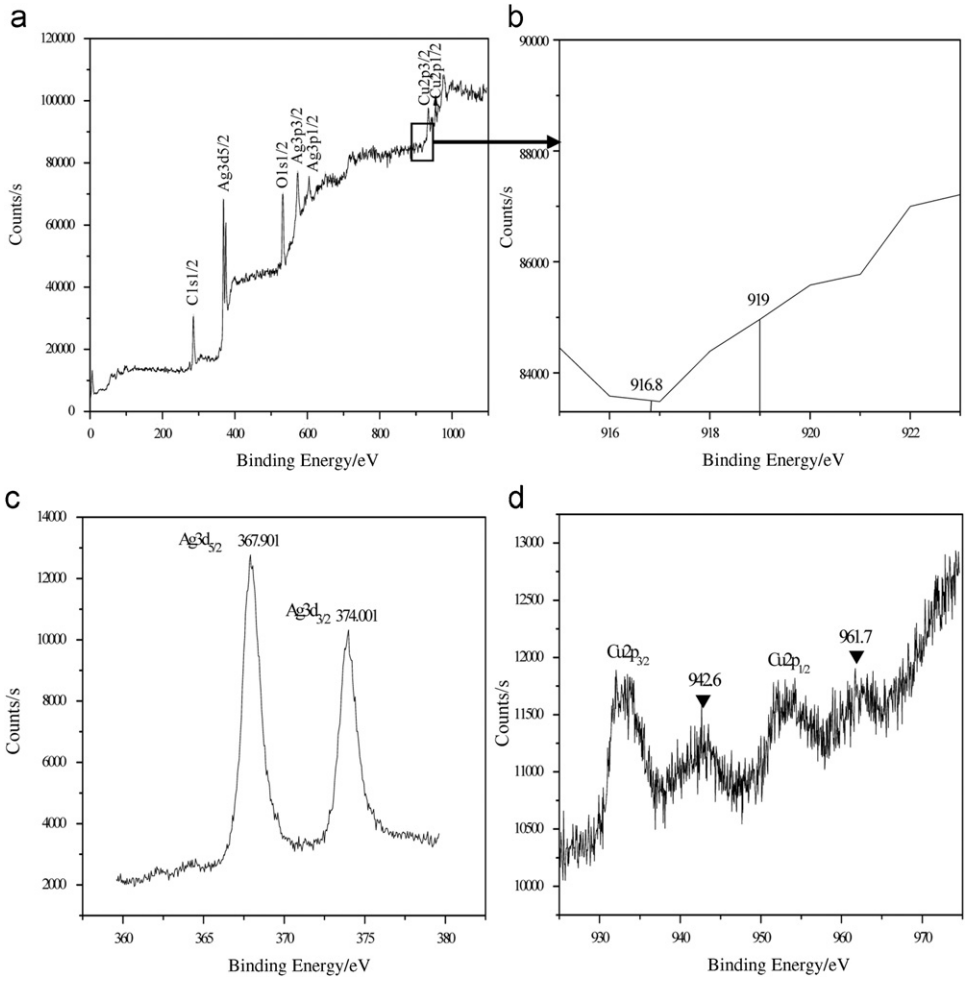

Fig. 7. (a) XPS spectra of Cu–Ag powders, (b) enlarged Cu Auger spectra in selected area of (a), (c) XPS spectra of Ag, and (d) XPS spectra of Cu.

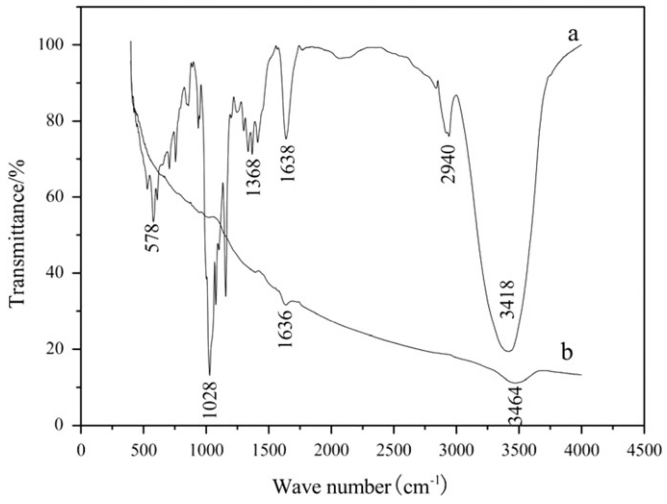

Fig. 8. FT-IR spectra of (a) pure β-CD and (b) Cu–Ag composite particles.

spectrum in Fig. 7a selected area that there is no peak at 916.8 eV; in contrast the peak at 919 eV is stronger, which shows there is no Cu_2O. The reason is that Cu_2O can be oxidized to CuO when there is enough Ag^+ in the solution. Finally, the oxidation of copper is to CuO. This suggests the Cu atoms on the surface are partially oxidized to CuO when most of particle surface is covered by Ag. CuO is not detected by XRD because of its too little amount.

3.3. Growth mechanism of Cu–Ag nanoparticles and role of β-CD

In order to study the effects of β-CD, FT-IR spectra are shown in Fig. 8. The characterized transmittance bands of β-CD at 946 cm^{-1} (skeletal vibration involving a-1,4 linkage), 756 cm^{-1} (ring 'breathing' vibration), 707 cm^{-1} (pyranose ring vibration), and 578 cm^{-1} (pyranose ring vibration) [25] disappeared (Fig. 8a). In Fig. 8b only two weak transmittance bands at 1028 and 3464 cm^{-1} were found, which are consistent with the flexural and stretching vibrations of –OH in H_2O, respectively. It can therefore be concluded that the β-CDs were washed away by deionized water. No β-CDs were found to exist in the Cu–Ag composite.

The stabilization of apolar Rh nanoparticles [26] and Pd colloids [27] by the hydrophobic cavities of CDs has been reported. However, the stabilization and resulting small dimensions as a result of the inclusion of the large nanoparticles in the CDs cavity are impossible. The diameter of particles obtained in this experiment is in the range of 100–150 nm, implying that β-CDs and Cu cannot form inclusion complexes because the particle sizes far exceed those of the β-CD cavities. This occurs because the effect of rapid growth of copper particles exceeds that of the critical particle that can be included by β-CD. Therefore, the good dispersity of Cu nanoparticle in the presence of CDs is more likely attributed by the hydrophobic interactions between the hydrophobic cavity of the β-CDs and the

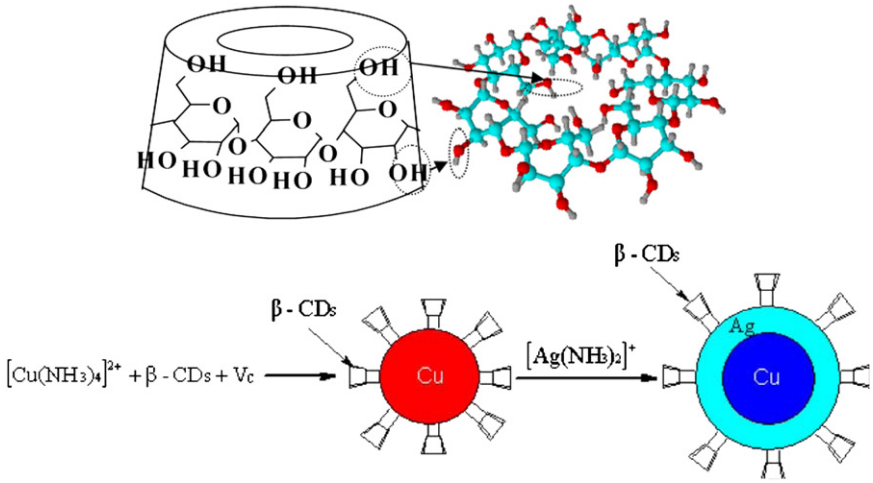

Fig. 9. Structures of β-CD and Cu–Ag bimetallic powder formation.

Cu particles, rather than formation of inclusions of Cu atoms or small Cu nanoparticles in the CD cavities [28]. CDs are conical torus-like macrocycles (Fig. 8) built from glucopyranose units. Their interior cavities, as well as the primary faces (small rings), are hydrophobic, while their secondary faces (large rings) and exterior surfaces are hydrophilic [29]. Therefore, the large Cu particles obtained in this study cannot fit into the CD cavities, but they can be chemisorbed on top (small ring) of the CD cavities to form other complexes through –OH bonding with Cu particles [30]. Because of such hydrophobic interactions with Cu nanoparticles they are less likely to agglomerate with other nanoparticles due to steric hindrance, which is similar to conventional surfactants and capping ligands. This results in smaller dispersed particles. The process is shown in Fig. 9.

4. Conclusions

Ag-coated Cu powders less than 150 nm in size were successfully synthesized by successive ascorbic acid reduction of metal salts in aqueous system. The resistance to oxidation is improved by increasing Ag content. As the molar ratio of Ag/Cu approached 1:1, a uniform and dense Ag coating was obtained. TEM observations showed that the Cu–Ag particles do not have clear core–shell regions. In the synthesized process, hindrance of β-CDs played an important role in avoiding aggregation of Cu–Ag composite particles through –OH bonding with Cu particles. Studies of the conductivity of the core–shell nanoparticles will be performed in the future.

Acknowledgment

This work is supported by the National High Technical Projects of China (2008AA03Z206) and National Natural Science Foundation of China (A3 Foresight Program-50821140308).

References

[1] B.K. Park, D. Kim, S. Jeong, J. Moon, J.S. Kim, Thin Solid Films 515 (2007) 7706.
[2] N.A. Luechinger, E.K. Athanassiou, W.J. Stark, Nanotechnology 19 (2008) 445201.
[3] Y. Lee, J. Choi, K.J. Lee, N.E. Stott, D. Kim, Nanotechnology 19 (2008) 415604.
[4] A. Sarkar, T. Mukherjee, S. Kapoor, J. Phys. Chem. C 112 (2008) 3334.
[5] B.C. Ranu, A. Saha, R. Jana, Adv. Synth. Catal. 349 (2007) 2690.
[6] E.K. Athanassiou, R.N. Grass, W.J. Stark, Nanotechnology 17 (2006) 1668.
[7] Y. Leroux, J.C. Lacroix, C. Fave, G. Trippe, N. Felidj, J. Aubard, A. Hohenau, J.R Krenn, ACS Nano. 2 (2008) 728.
[8] N. Cioffi, L. Torsi, N. Ditaranto, G. Tantillo, L. Ghibelli, L. Sabbatini, T.B. Zacheo, M.D. Alessio, P.G. Zambonin, E. Traversa, Chem. Mater. 17 (2005) 5255.
[9] X. Zhang, G. Wang, X. Liu, H. Wu, B. Fang, Cryst. Growth Des. 8 (2008) 1430.
[10] P.S. Ghosh, C.K. Kim, G. Han, N.S. Forbes, V.M. Rotello, ACS Nano 2 (2008) 2213.
[11] H.T. Hai, J.G. Ahn, D.J. Kim, et al., Surf. Coat. Technol. 201 (2006) 3788.
[12] E. Takeshima, K. Takatsu, Y. Kojima, T. Fujji, US Patent 235(1990) 954.
[13] S.tojan Djokic, M. Dubois, R.H. Lepard, US Patent 158 (1999) 945.
[14] T. Hayashi, Shimonoseki, US Patent 178 (1993) 909.
[15] Xinrui Xu, Xiaojun Luo, Hanrui Zhuang, Wenlan Li, Baolin Zhang, Mater.Lett. 57 (2003) 3987.
[16] D.M. Makowiecki, J.A. Kerns, C.S. Alford, M.A. Mckernan, US Patent B1, 355 (2002) 146.
[17] J. Liu, S. Mendoza, E. Roman, M.J. Lynn, R. Xu, A.E. Kaifer, J. Am. Chem. Soc. 121 (1999) 4304.
[18] J. Alvarez, J. Liu, E. Roman, A.E. Kaifer, Chem. Commun., Cambridge, UK, 2000 1151.
[19] S. Giuffrida, G. Ventimiglia, S. Petralia, S. Conoci, S. Sortino, Inorg. Chem. 45 (2006) 508.
[20] W. Sänger, J. Jacob, K. Gessler, T. Steiner, D. Hoffmann, H. Sanbe, K. Koizumi, S.M. Smith, T. Takaha, Chem. Rev. 98 (1998) 1787.
[21] Y. Liu, K.B. Male, P. Bouvrette, J.H.T. Luong, Chem. Mater. 15 (2003) 4172.
[22] D. Bonacchi, A. Caneschi, D. Gatteschi, C. Sangregorio, R. Sessoli, A.J. Falqui, Phys. Chem. Solids 65 (2004) 719.
[23] B. He, J.J. Tan, K.Y. Liew, H.J. Liu, Mol. Catal. A 221 (2004) 121.
[24] T.S. Anderson, R.H. Magruder III, J.E. Wittig, et al., Nucl. Instrum. Methods Phys. Res. B 171 (2000) 401.
[25] O. Egyed, Vibr. Spectrosc 1 (1990) 225.
[26] M. Komiyama, H. Hirai, Bull. Chem. Soc. Jpn. 56 (1983) 2883.
[27] I. Wilner, D.J. Mandler, Am. Chem. Soc 111 (1989) 1330.
[28] Szejtli, J. Chem. Rev. 98 (1998) 1743.
[29] C.H.B. Ng, J. Yang, W.Y. Fan, J. Phys. Chem. C 112 (2008) 4141.
[30] Huang Yunjie, Li Di, Li Jinghong, Chem. Phys. Lett. 389 (2004) 14.